INTERNATIONAL JOURNAL OF ACADEMIC RESEARCH IN ECONOMICS & MANAGEMENT SCIENCES

OPEN ACCESS JOURNAL

Vol 14, Issue 4, (2025) E-ISSN: 2226-3624

Effect of pH-Controlled Titanium Dioxide Synthesis on Solar Cell Performance and its Relevance to Renewable Energy Economics

Nur Alfarina Pirdaus[1], Muhammad Azfar Shamil Abd Aziz[1], Nurfadzilah Ahmad[1*], Ishak Annuar[2]

[1]Solar Research Institute (SRI), Universiti Teknologi MARA (UiTM) Shah Alam, Selangor,

[2]Faculty of Electrical Engineering, Universiti Teknologi MARA (UiTM) Sarawak, Kampus Samarahan

Corresponding Author Email: nurfadzilah6344@uitm.edu.my

DOI Link: http://dx.doi.org/10.6007/IJAREMS/v14-i4/26607

Published Online: 12 October 2025

Abstract

Titanium dioxide (TiO2) is a transparent to visible light n-type wide band gap semiconductor. Employing a wide band gap semiconductor and sensitizer dyes adsorbed on it, Dye-sensitized Solar Cell (DSSC) can convert visible light into electrical energy. TiO2 paste in this study was prepared using TiO2 powder synthesized by the sol- gel method with differing pH values. The comparison study on the phase, morphological, and optical characterizations of thin films of these TiO2 pastes was carried out using 2-Point Probe, X-ray diffraction (XRD), Field-Emission Scanning Electron Microscope (FESEM), and Ultraviolet-visible (UV–vis) spectroscopy in this study. The XRD pattern detects the occurrence of the amorphous phase of TiO2- structured thin films in all thin films. FESEM images show that TiO2 with pH4 and pH6 consists of less agglomerated particle distribution compared to pH8, which may impede photocatalytic activity. The bandgap energy of TiO2 thin films was 2.25 eV, 2.15 eV, and 1.56 eV at pH4, pH6, and pH8, respectively. A pH of 6 is optimum in sol-gel synthesis as it facilitates a balanced hydrolysis and condensation rate, resulting in a consistent, pre- ordered amorphous gel network that can effectively crystallize into a pure anatase structure. This study is novel in its emphasize correlation of sol–gel synthesized TiO_2 at different pH values, which shows that pH has a significant impact on surface morphology, optical bandgap, and particle agglomeration. These factors essential to dye adsorption and electron transport in DSSC applications. The results obtained suggest improvement on the coating method for better optimization for DSSC application.

Keywords: Solar Cell, DSSC, Titanium Dioxide (TiO_2), pH, Sol-gel

Introduction

Compared to other semiconducting metal oxides, titanium dioxide (TiO_2) is a promising semiconductor material with a wide range of applications due to its good optical and electrical properties, non-toxicity, and high stability for photocatalytic applications. TiO_2

is primarily attractive because of its low cost of manufacture, ease of handling, and non-toxicity (Dubey et al., 2019). Their application varies based on their properties. Due to its light scattering capabilities, high refractive index, and ultraviolet (UV) absorptivity, rutile TiO_2 is widely employed as a pigment, opacifier, isolator, and in switches, among other things, whereas anatase TiO_2 is favoured for photovoltaic and photocatalytic applications.

Three polymorphisms of the semiconductor TiO_2 exist: rutile, anatase, and brookite (Dubey et al., 2019). In contrast to other phases like brookite and TiO_2 (B) monoclinic, the anatase and rutile crystalline phases of TiO_2 are mostly required for industrial purposes. The crystalline phases of rutile and anatase have energy band gaps of 3.0 eV and 3.2 eV, respectively. Because anatase-TiO_2 has a high electron mobility, dye-sensitized solar cells (DSSCs) use it as the photoanode material. The selection of anatase-TiO_2 demonstrated a reasonable increase in cell efficiency (Yeoh et al., 2023). The anatase phase, due to its smaller particle sizes, is the most thermodynamically stable state (Keshari et al., 2022).

Sputtering, chemical vapour deposition (CVD), pulsed laser deposition (PLD), electrophoretic deposition (EPD), magnetron sputtering, thermal evaporation, and the sol–gel spin coating method are among the deposition methods for TiO_2 thin films. Because sol–gel spin coating is a simple, economical, and adaptable method, it is frequently used to fabricate thin films (Devi et al., 2022). The sol–gel technique has the benefit of producing stable surfaces and optimal surface area (Ibrahim & Sreekantan, 2010). The two phases of the sol–gel process are: (a) the hydrolysis of precursors with organometallic components; and (b) the polycondensation of the hydrolysed products (Ibrahim & Sreekantan, 2010). Moreover, TiO_2 nanostructure has been studied for flexible uses in future applications (Keshari et al., 2022). This process, as opposed to other chemical processes, yields tiny particles with distinct physical features. The low temperature and pressure process of the sol–gel approach makes it simple. With this technology, one can adjust the composition and microstructural characteristics of the nanoparticles with flexibility, contingent on the precursor's chemistry and the synthesis conditions (Dubey et al., 2019).

Despite being primarily produced using sol–gel synthesis, research on the pH alteration using both acid and base catalysts and their effects on the structural, morphological, and optical aspects of TiO_2 are still not fully discovered. In this study, TiO_2 was prepared using the sol–gel method with titanium (IV) butoxide as a precursor, ethanol as a solvent, and the addition of HCl and NaOH as catalysts for pH adjustment. The effect of pH adjustment on the structural, morphological, and optical properties of TiO_2 thin films was studied for optimization in DSSC application.

Experimental Procedures

Preparation of TiO_2 Nanoparticles by the Sol-Gel Method

The reagents used are all analytical grade, and they have not been further purified. To create the sol-gel synthesized TiO2, 10 ml of titanium (IV) butoxide was dissolved in absolute 10 ml of ethanol and agitated for an hour. 5 ml of distilled water was then gradually added dropwise to the solution. Nearly immediately, the ensuing gel was created, and it was stirred for a few minutes. The solution was rapidly stirred for an hour to generate white colloidal precipitate after the pH had been corrected with 1 mole of NaOH or HCl to vary the solution

pH from pH4 to pH8. pH4, pH6 and pH8 were chosen in this experiment to study different range of pH condition which are highly acidic, mild acidic (near neutral) and basic.

After 24 hours, the solutions were filtered. In order to evaporate as much water and organic material as possible, they were then spent the final 12 hours in an oven set at 100°C. After drying, the material will be milled into a fine powder using a ball mill machine for 2 hours. Figure 1. shown the simplified process flow of TiO_2 sol-gel synthesis.

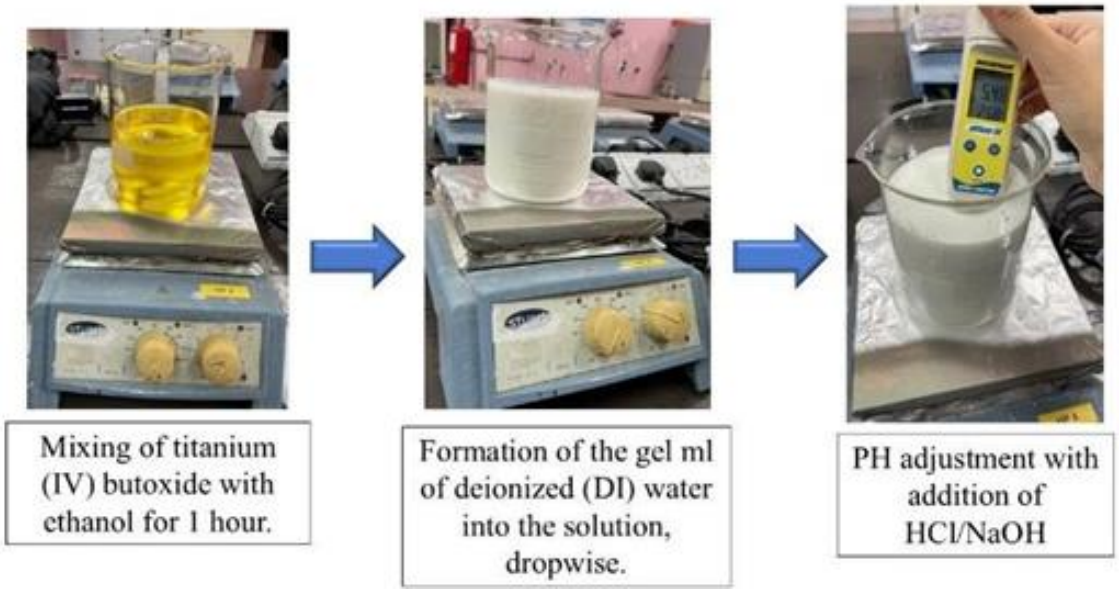

Figure 1. Process flow of TiO_2 sol-gel synthesis

Preparation of TiO_2-Coated Thin Film

2 g of the prepared TiO2 powder was added to 100 ml of ethyl alcohol and stirred for 30 minutes to form a homogenous TiO2 paste. Before usage, the solution was kept in the dark. The glass substrate was cleaned in a sonicator for 15 minutes alternately with ethanol and deionised water before coating. 10 drops of TiO2 paste were dropped onto the dried and cleaned glass substrates at a speed of 3000 rpm to create a single layer of coating. The glass substrate was then dried at 100°C for 10 minutes. The same technique was repeated for second and third layer of coating. The final coating underwent a 30-minute annealing at 500°C.

Characterization

FESEM was utilised for analyzing the surface morphology of TiO_2 while UV-Visible spectrometer was used to evaluate the transmittance and bandgap energy of both types of TiO_2 at the 300 nm to 800 nm range. X-ray diffraction (XRD) was used to identify the phase of the thin film spin coated with different PHs and 2-point probe was used to measure the current-voltage for electrical properties analysis.

Results and Discussion

Electrical Properties

Fig. 2 shows the current-voltage (I-V) characteristics of the TiO_2 thin films with different pHs. The current was measured with voltage values from –10 V to 10 V. From the result, it can be concluded that the TiO_2 samples exhibit a linear and symmetrical curve, indicating ohmic contact characteristics between the thin films and the gold metal contact. The slope of the

curve is observed to become steeper with the increase in pH. The sample at pH 8 showed the steepest slope, followed by pH 6 and pH 4.

TiO_2 thin film with pH 8 exhibited the highest current (9.23×10^{-9} A) at 10 V, followed by pH 6 (8.27×10^{-9} A) and pH 4 (6.16×10^{-9} A). The I-V curves provide valuable insights into the photoelectrochemical performance of DSSCs, revealing how the pH of the TiO_2 thin film influences the device's efficiency and charge transport characteristics.

The material may produce an internal voltage and current if the measurement is done in an illuminated environment. This is the basic idea of solar cells. Photon absorption can produce electron–hole pairs, which can result in a detectable current (short-circuit current, or ISC_{SC}SC) even in the absence of an external voltage (V = 0). The opposite is also true: an open-circuit voltage, or reverse bias voltage, must be provided in order to push the current to zero (I = 0). With intercepts on both the x and y axis, this causes the I-V curve to go into the second and fourth quadrants (Lindholm et al., 1979).

The high conductivity of the amorphous structure is not due to the perfect band transport of electrons as in a crystal. Rather, conduction frequently takes place via mechanisms that depend on defect states. At pH 6, the anatase phase forms under ideal conditions, resulting in a more stoichiometric and organized TiO_2 structure. Despite being a semiconductor, anatase's crystalline, low-defect nature usually leads to a lower intrinsic conductivity and a wider band gap (~3.2 eV) than a non-stoichiometric amorphous film with numerous conductive defect states (Stiller et al., 2017).

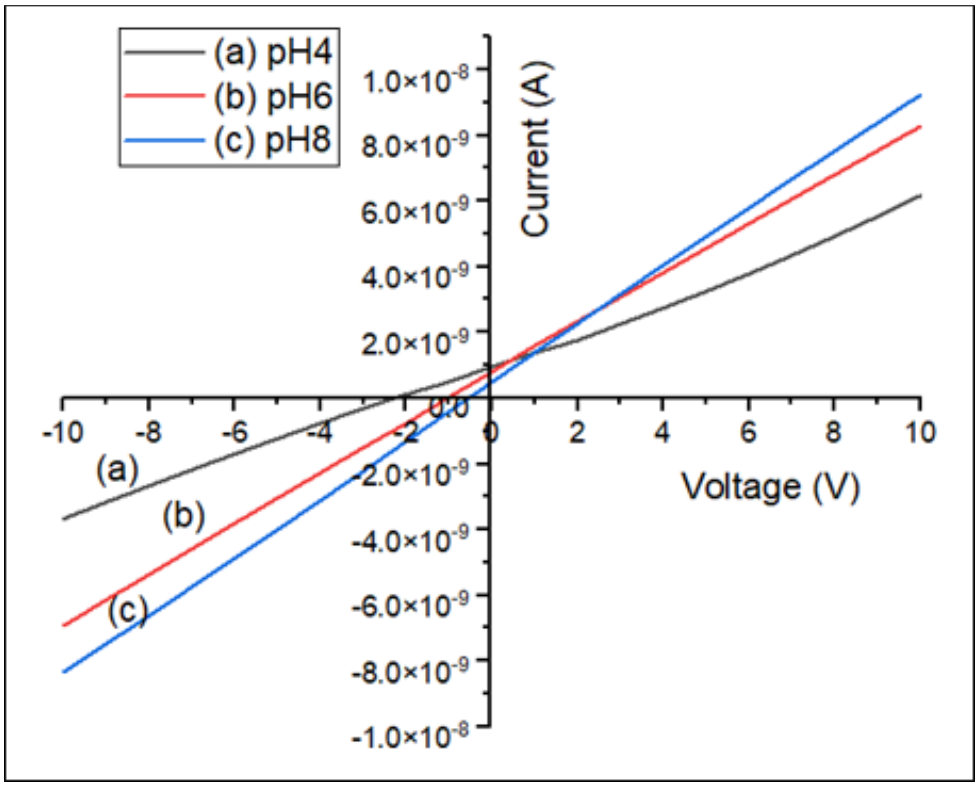

Figure 2. I-V measurement plots of TiO_2 thin films with 3 different pH (a) pH4 (b) pH6 (c) pH8

Table 1
Average resistivity and conductivity of 3 different pH; pH4, pH6, and pH8

pH of TiO_2	Average Resistivity (Ω.m)	Average Conductivity (Siemen's/m)
pH4	5.7932	$1.72616x10^{-10}$
pH6	4.4597	$2.2323x10^{-10}$
pH8	4.1241	$2.42477x10^{-10}$

Optical Properties

Figure 3 exhibits the optical transmittance spectra of 3 different pHs of TiO2 photoanode with wavelengths ranging from 300 to 800 nm. The transmittance of the three samples showed an increasing transmittance with only a small increase. pH4 TiO2 exhibited the highest transmittance compared to the other pHs, with 90% maximum transmittance, followed by pH6 with 85% transmittance. Meanwhile, pH8 only exhibits transmittance below 50%. It can be seen that transmittance values decrease as pH increases. Low transmittance might be due to the dense and compact structure of the TiO2 film crystalline structure which reduces its transparency. This structure can be seen in the FESEM images of TiO2 powder synthesized by sol-gel method (Figure 6) from Section 3.4.

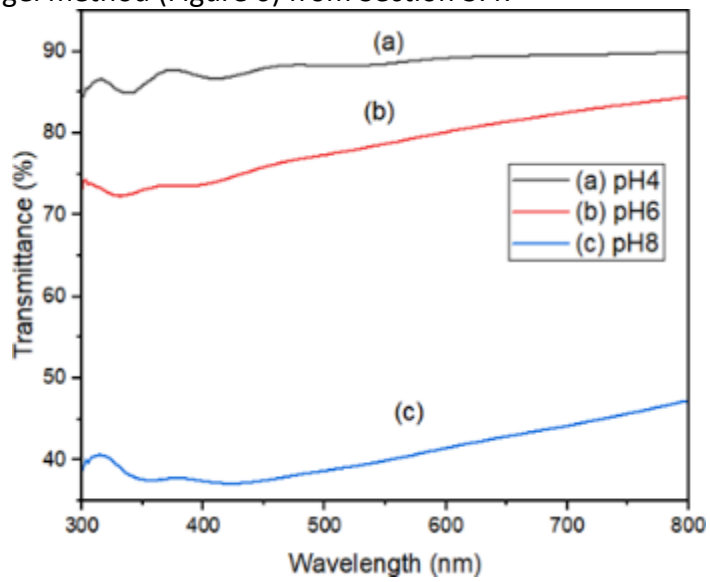

Figure 3. Transmittance spectra of TiO_2 thin films with 3 different pH (a) pH4 (b) pH6 (c) pH8

Beer-Lambert law was used to estimate the optical band gap energy (Eg) based on the absorbance spectra obtained from UV-Vis- NIR characterization, and this Tauc plot was used to calculate the optical band gap (Eg) using the equation below:

$$\alpha h\nu = A(h\nu - Eg)^n \quad (1)$$

Where:
α= absorption coefficient
Eg= nanoparticle band gap valu
$h\nu$= energy of the photon
A= constant associated with the effective masses of the bonds
n= denotes the transition nature; n = 2 corresponding to the allowed direct transitions while n = ½ corresponding to indirect transitions. It was estimated by extrapolating the linear portion of the $(\alpha h\nu)^2$ vs. photon energy curve to the photon energy axis (Priyalakshmi Devi et al., 2022). The Tauc plot of TiO_2 thin films with different pHs is shown in Figure 4. The bandgap energies for pH 4, pH 6, and pH 8 are 2.25 eV, 2.15 eV, and 1.56 eV, respectively. The decrease

in band gap with increasing pH can be correlated to the reduction of the crystallite size that determines the quantum size effect, which induces a blue shift of the absorption edge in the optical reflectance. Lowering of pH gave an obvious decrease in the crystallite size that can be correlated with the increase of the band gap (Tsega & Dejene, 2017).

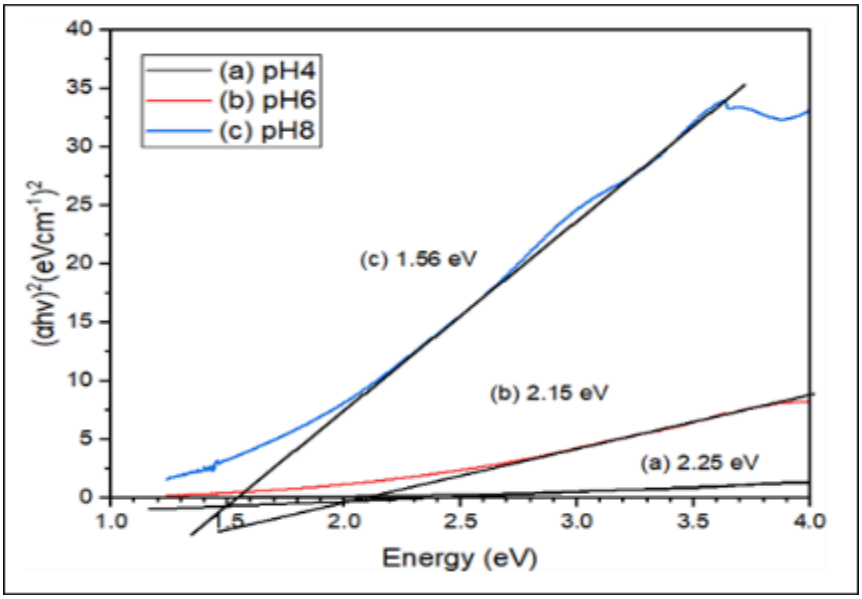

Figure 4. Tauc plot of TiO_2 thin films with 3 different pH (a) pH4 (b) pH6 (c) pH8

Structural Properties

XRD characterizations were carried out to identify the phase composition of the TiO_2 powders from the sol–gel synthesized with different pHs, and the resulting diffraction pattern was plotted as shown in Figure 5, with measurement ranges from 10° to 90°. From the XRD pattern, a peak started to form at around 20° for all five samples, but only the TiO_2 powder with pH 6 formed a sharp peak instead of a broadening peak like in the TiO_2 powders with pH 4 and pH 8.

The XRD pattern of TiO_2 powder with pH 6 indicates the formation of the anatase phase, while the broadening peaks for the others represent the formation of the amorphous phase. The observed anatase peaks are located at 25.31°, 37.88°, 48.03°, 53.98°, 55.06°, and 62.74°, which are assigned to the (101), (112), (200), (105), (211), and (204) planes, respectively. They are in good agreement with the standard spectrum (JCPDS No.: 00-064-0863) (Low et al., 2021). Indeed, anatase has been shown to work as an indirect semiconductor, where electron deexcitation from the conduction band to the valence band is forbidden by selection criteria. Therefore, anatase has a greater electron–hole lifetime than rutile, a direct semiconductor with a lower carrier lifetime (Low et al., 2021).

In general, the sol–gel generated precipitates in the sol–gel technique are amorphous in nature and additional heat treatment is needed for crystallization. To cause the transition from amorphous to anatase phase, an annealing temperature of more than 300 °C is usually necessary, resulting in a substantial increase in particle size. Titania's photocatalytic activity, on the other hand, is affected by particle size as well as crystallinity (Ibrahim & Sreekantan, 2010). Due to its less limited structure and improved formation kinetics, anatase is the favored phase for production during TiO_2 synthesis (Yeoh et al., 2023). A balanced rate of

hydrolysis and condensation is frequently provided by an intermediate pH, such as pH 6. In contrast to very acidic and basic pH, where the hydrolysis rate may be too high—resulting in rapid precipitation and the formation of a highly disordered, amorphous gel network—this enables the formation of a more controlled, less aggregated, and more ordered polymeric network or smaller, more uniform nanoparticles within the gel, which facilitates the formation of a pure anatase phase.

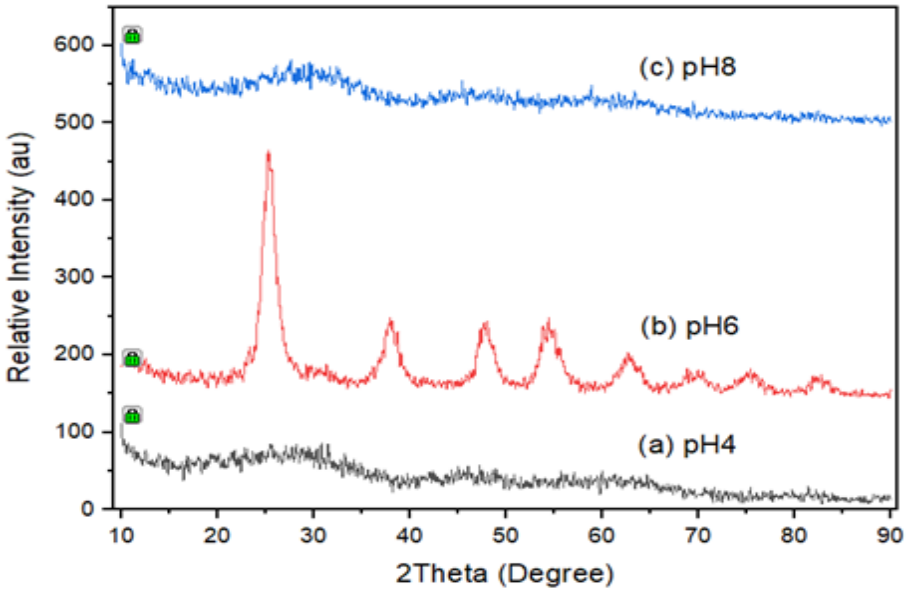

Figure 5. XRD spectra of TiO_2 thin films with 3 different pH (a) pH4 (b) pH6 (c) pH8

Morphological Properties

The FESEM images of the TiO_2 powders with pH 4, pH 5, pH 6, and pH 8 under 5000× magnification presented in Figure 6 show that all samples exhibited an irregular shape morphology and were agglomerated. There were no obvious differences observed between the morphology of the different pHs of TiO_2 powders. From the FESEM images, pH 6 exhibited a more compact structure compared to pH 4, pH 5, and pH 8. The increase in crystallite size is directly correlated with the tendency of particle agglomeration. The precursor solution's pH condition has a significant impact on the morphology (Tsega & Dejene, 2017). The changes in pH of the synthesized TiO_2 powders influence the variation in particle size. The morphology of TiO_2 is significantly influenced by pH levels; as the pH value increases, the particles decrease in size and become more agglomerated.

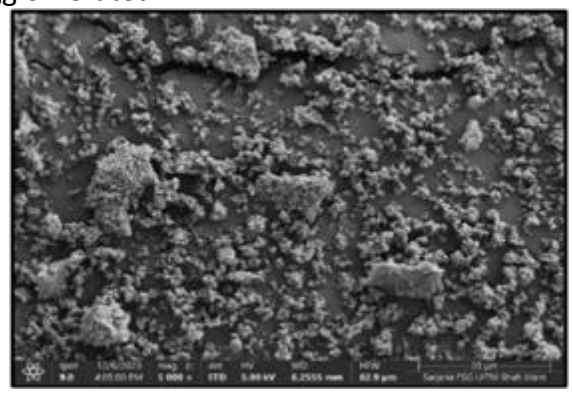

(a)

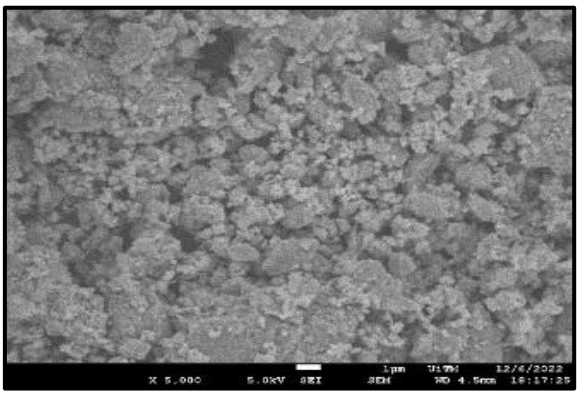

(b)

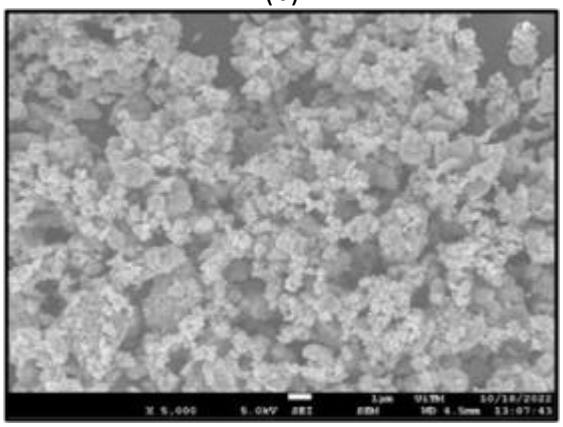

(c)

Figure 6. FESEM images of TiO_2 powder synthesized by sol-gel method with (a) pH4 (b) pH5 (c) pH6 (d) pH8 under 5000X magnification

The presence of titanium (Ti) and oxygen (O) elements in the sample was determined by the EDX spectrum. The percentage of the atomic content is displayed in Figure 7. Ti and O had respective atomic contents of 76.2% and 23.8%. These EDX results confirm the presence of TiO_2 particles that were successfully synthesized by the sol-gel method (Mortezaali & Yousefi, 2016).

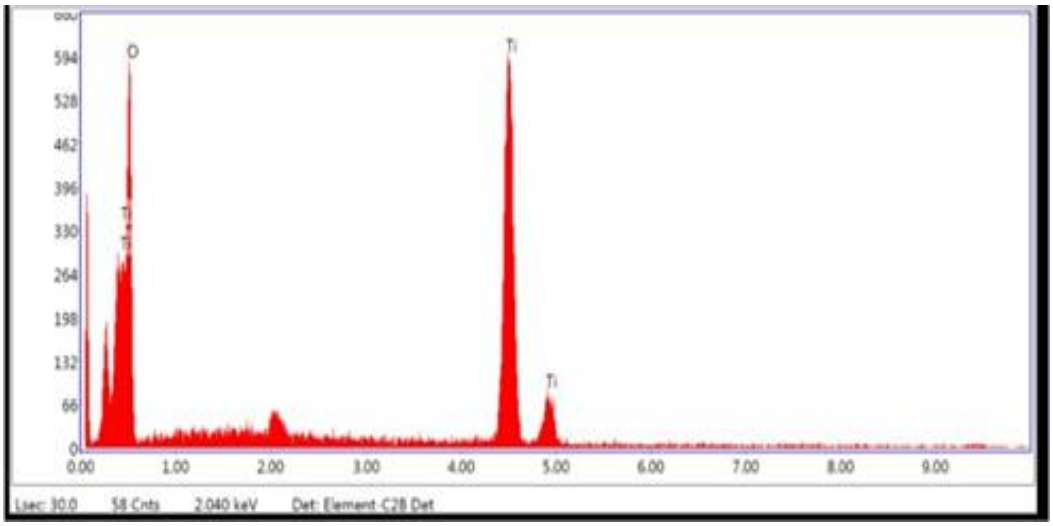

Figure 7. EDX spectrum of TiO_2 powder synthesized by the sol-gel method

Conclusion

The objectives of this research were to determine how the pH of TiO2 synthesized by the sol-gel method affected the morphological, structural, optical, and electrical properties of the TiO2 photoanode utilised in dye-sensitized solar cells (DSSCs) and their performance. This can be attributed to the enhanced dye absorption capability of the photoanode. The results obtained showed that the adjustment of the TiO_2 photoanode's pH do affect the crystallinity, surface roughness, porosity, and bandgap. Prominently, an optimal pH level, which in this case, pH6, significantly improved dye-loading capacity by increasing surface area and improving pore structure, which in turn boosted light harvesting and electron transport efficiency. These revelations present a viable avenue for more sol-gel parameter tuning in order to design photoanodes with specific characteristics for high- efficiency DSSCs. To further improve cell performance and long-term stability, future research could investigate combining pH-optimized TiO_2 with co-sensitization tactics, surface passivation methods, or plasmonic nanostructure inclusion.

Acknowledgements

The authors would like to thank the Ministry of Higher Education (MOHE) under grant FRGS/1/2021/TK0/ UITM/02/12 for the financial support and Solar Research Institute (SRI), NANO- Electronic Centre, School of Electrical Engineering, School of Mechanical Engineering and Faculty of Applied Science of Universiti Teknologi MARA (UiTM) for facilities support.

References

Agarwal, R., Vyas, Y., Chundawat, P., Dharmendra, & Ameta, C. (2021). Outdoor performance and stability assessment of dye-sensitized solar cells (DSSCs). In M. Aghaei (Ed.), *Solar radiation* (Ch. 7). IntechOpen. https://doi.org/10.5772/intechopen.98621

Ali, F. H., & Alwan, D. B. (2018). Effect of particle size of TiO_2 and additive materials to improve dye sensitized solar cells efficiency. *Journal of Physics: Conference Series, 1003*(1), 012077. https://doi.org/10.1088/1742-6596/1003/1/012077

Ammar, A. M., Mohamed, H. S. H., Yousef, M. M. K., Abdel-Hafez, G. M., Hassanien, A. S., & Khalil, A. S. G. (2019). Dye-sensitized solar cells (DSSCs) based on extracted natural dyes. *Journal of Nanomaterials, 2019*(1), 1867271. https://doi.org/10.1155/2019/1867271

Cabezuelo, O., Diego-Lopez, A., Atienzar, P., Marin, M. L., & Bosca, F. (2023). Optimizing the use of light in supported TiO_2 photocatalysts: Relevance of the shell thickness. *Journal of Photochemistry and Photobiology A: Chemistry, 444,* 114917. https://doi.org/10.1016/j.jphotochem.2023.114917

Dubey, R. S., Krishnamurthy, K. V., & Singh, S. (2019). Experimental studies of TiO_2 nanoparticles synthesized by sol-gel and solvothermal routes for DSSCs application. *Results in Physics, 14,* 102390. https://doi.org/10.1016/j.rinp.2019.102390

Ekar, S. U., Shekhar, G., Khollam, Y. B., Wani, P. N., Jadkar, S. R., Naushad, M., Chaskar, M. G., et al. (2017). Green synthesis and dye-sensitized solar cell application of rutile and anatase TiO_2 nanorods. *Journal of Solid State Electrochemistry, 21*(9), 2713–2718. https://doi.org/10.1007/s10008-016-3376-3

Elsaeedy, H. I., Qasem, A., Yakout, H. A., & Mahmoud, M. (2021). The pivotal role of TiO_2 layer thickness in optimizing the performance of TiO_2/P-Si solar cell. *Journal of Alloys and Compounds, 867,* 159150. https://doi.org/10.1016/j.jallcom.2021.159150

Elshimy, H., Abdallah, T., & Abou Shama, A. (2020). Optimization of spin coated TiO_2 layer for hole-free perovskite solar cell. *IOP Conference Series: Materials Science and Engineering, 762*(1), 012003. https://doi.org/10.1088/1757-899X/762/1/012003

Jeng, M. J., Wung, Y. L., Chang, L. B., & Chow, L. (2013). Particle size effects of TiO_2 layers on the solar efficiency of dye-sensitized solar cells. *International Journal of Photoenergy, 2013*(1), 563897. https://doi.org/10.1155/2013/563897

Kazim, O. S., & Nwauzor, J. N. (2020). Analysis of fabrication, characterization and performance of dye-sensitized solar cell using natural dye. *International Journal of Advancement in Development Studies,* 43–57. https://www.researchgate.net/publication/364330633

Lallo, A. I. M. J., Prima, E. C., Suhendi, E., & Yuliarto, B. (2022). Effect of TiO_2 thin film thickness and dye characterization using binahong leaf (*Anredera cordifolia*) as photosensitizer in dye-sensitized solar cell. *Journal of Aceh Physics Society, 11*(4), 109–114. https://doi.org/10.24815/jacps.v11i4.28302

Mary, N. T., Rosana, Amarnath, J., Joseph, V. K. L., Suresh, A., Sambandam, A., & Reddy, S. (2014). Natural sensitizers for dye sensitized solar cell applications. *International Journal of Scientific & Engineering Research, 5*(3), 340–344. https://www.researchgate.net/publication/264045910

Nadzirah, S., & Hashim, U. (2013). Annealing effects on titanium dioxide films by sol-gel spin coating method. In *Proceedings - RSM 2013: IEEE Regional Symposium on Micro and Nano Electronics* (pp. 159–162). IEEE. https://doi.org/10.1109/RSM.2013.6706497

Swathi, K. E., Jinchu, I., Sreelatha, K. S., Sreekala, C. O., & Menon, S. K. (2018). Effect of microwave exposure on the photo anode of DSSC sensitized with natural dye. *IOP Conference Series: Materials Science and Engineering, 310*(1), 012141. https://doi.org/10.1088/1757-899X/310/1/012141

Tanihaha, S. L., Uranus, H. P., & Darma, J. (2010). Fabrication and characterization of dye-sensitized solar cell using blackberry dye and titanium dioxide nanocrystals. In *Proceedings - 2010 2nd International Conference on Advances in Computing, Control and Telecommunication Technologies (ACT 2010)* (pp. 60–63). IEEE. https://doi.org/10.1109/ACT.2010.46

Theivasanthi, T., & Alagar, M. (2013). Titanium dioxide (TiO_2) nanoparticles XRD analyses: An insight. *arXiv.* http://arxiv.org/abs/1307.1091

Wu, S., Luo, X., Long, Y., & Xu, B. (2019). Exploring the phase transformation mechanism of titanium dioxide by high temperature in situ method. *IOP Conference Series: Materials Science and Engineering, 493*(1), 012010. https://doi.org/10.1088/1757-899X/493/1/012010

Zainol, M. N. B., & Mamat, M. H. (2017). Content variation of particle size in TiO_2 paste as medium for electron transportation in dye sensitized solar cell. In *Proceedings - 14th IEEE Student Conference on Research and Development (SCOReD 2016): Advancing Technology for Humanity.* IEEE. https://doi.org/10.1109/SCORED.2016.7810081